

1992

## The Incorporation of Glass-Ceramic Implants in Bone after Surface Conditioning Glow-Discharge Treatment

C. M. Muller-Mai  
*Freie Universitat Berlin*

C. Voigt  
*Freie Universitat Berlin*

R. E. Baier  
*State University of New York, Buffalo*

U. M. Gross  
*Freie Universitat Berlin*

Follow this and additional works at: <https://digitalcommons.usu.edu/cellsandmaterials>



Part of the [Biomedical Engineering and Bioengineering Commons](#)

---

### Recommended Citation

Muller-Mai, C. M.; Voigt, C.; Baier, R. E.; and Gross, U. M. (1992) "The Incorporation of Glass-Ceramic Implants in Bone after Surface Conditioning Glow-Discharge Treatment," *Cells and Materials: Vol. 2 : No. 4* , Article 5.

Available at: <https://digitalcommons.usu.edu/cellsandmaterials/vol2/iss4/5>

This Article is brought to you for free and open access by the Western Dairy Center at DigitalCommons@USU. It has been accepted for inclusion in Cells and Materials by an authorized administrator of DigitalCommons@USU. For more information, please contact [digitalcommons@usu.edu](mailto:digitalcommons@usu.edu).



## THE INCORPORATION OF GLASS-CERAMIC IMPLANTS IN BONE AFTER SURFACE CONDITIONING GLOW-DISCHARGE TREATMENT

C.M. Müller-Mai\*, C. Voigt<sup>1</sup>, R.E. Baier<sup>2</sup>, U.M. Gross

Institute of Pathology, <sup>1</sup>Department of Traumatology and Reconstructive Surgery,  
Klinikum Steglitz, Freie Universität Berlin, Hindenburgdamm 30, 1000 Berlin 45, Germany;

<sup>2</sup>Department of Biomaterials, State University of New York, 323 Squire Hall, Buffalo, NY 14214, USA

(Received for publication September 2, 1992, and in revised form December 30, 1992)

### Abstract

Glow discharge (GD)-treated and autoclaved glass-ceramics of bone-bonding and non-bonding type were implanted into the femoral diaphysis of rats for 3, 7, 14 and 28 days and were investigated by applying light microscopy and histomorphometry, and scanning and transmission electron microscopy. More bone and chondroid, and faster osteoid development were observed at glow-discharge treated implants even in non-bonding implants when compared to autoclaved controls. Ultrastructural investigations showed a higher leaching-rate of GD-treated bone-bonding implants during the early days after implantation leading to a higher rugosity, whereas no morphological changes were observed on non-bonding implant surfaces. More extracellular matrix (ECM) forming productive cells and less macrophages were observed on GD-sterilized implant surfaces. Osteoclast-like cells were detected exclusively at 3 and 7 days post-operatively on GD-sterilized bone-bonding implants. The higher amount of bone at GD-treated surfaces was thought to be due to a higher leaching rate leading to higher surface-rugosity and interface alkalinity. Thus, GD-treatment seems to be suitable for sterilization of surface-reactive implants to yield earlier functionality and to reduce possible degradative processes.

**Key Words:** Bone, implant, glass-ceramic, glow-discharge, histology, ultrastructure, morphometry.

\*Address for correspondence:

C.M. Müller-Mai,  
Institute of Pathology,  
Freie Universität Berlin,  
Hindenburgdamm 30,  
1000 Berlin 45, Germany

Telephone number: 030 798-2296

### Introduction

The bond of bone to surface reactive materials, e.g., glass-ceramic KG Cera, is well established. These materials were mainly used in non load-bearing applications because they display poor mechanical properties. Many attempts have been made to improve these properties, e.g., by hot isostatic pressing of glass-ceramic and titanium particles and by coating of surface reactive materials onto a metal core. On one hand, due to the different thermal expansion of different materials, cracks in the hot isostatic pressed material can be induced and in the case of coatings, the outer bioactive component disrupted, especially when bending forces were also applied. On the other hand, if the interface of the surface-reactive component was not stabilized by bone-bonding, a partial disintegration of materials like glass-ceramic KG Cera or hydroxyapatite due to several processes was observed (Gross *et al.*, 1981, 1988; Müller-Mai *et al.*, 1990). Such processes led to degradation of the coating and therefore, might promote rupture between coating and substrate which might result in loss of the whole implant. Additionally, another aim, when using load-bearing implants, is to increase the interface resistance against load and to establish functional immobility of the implant as early as possible. Therefore, in an ideal case, a fast and total cover of bioactive implants or parts of implants with bone should reduce implant failure. Processes which promote and accelerate bone-bonding mechanisms are, therefore, of utmost importance and should be applied to improve the interface stability.

The implant surface plays a decisive role in the bony implantation bed since it is the first part of an implant which comes in contact with the tissue. Therefore, it is of utmost importance, that the final implant treatments do not adversely change the surface properties, i.e., in surface reactive implants, the mechanisms leading to bone-bonding or bone contact should not be inhibited, e.g., by surface contaminations. It was shown in former studies, that the process of sterilization influences the healing sequence of various kinds of implants e.g., by producing hydrophobic organic and hygroscopic salt contaminants on the implant surface by applying steam sterilization (Baier *et al.*, 1982). The influence

on the host response was related to the active surface properties such as the surface free energy, which was extrapolated from contact angle measurements (Baier, 1982; Baier *et al.*, 1986). The surface free energy was defined to be a measure of the extent of unsaturated bonds on the implant surface (Hench and Ethridge, 1982) and seems to be mainly due to weak, physical van der Waals bonds. High surface energies can be obtained by a glow-discharge (GD) sterilization procedure of implants. GD-treatment increases implant wettability, i.e., implants become more hydrophilic, since this procedure scrubs away any organic surface contamination by violently moving ionized gas particles (Baier *et al.*, 1975, Baier, 1982). Additionally, highly wettable surfaces yielded better attachment behaviour of cells *in vitro*. Cells grown on highly wettable glass *in vitro* needed much higher fluid shear force to cause detachment than hydrophobic teflon (Kooten van *et al.*, 1991).

Due to different implant surface properties, the amount and kind of adsorbed proteins and cells are influenced. It was shown in former studies that GD-treated surfaces with high energies, i.e., with better wettability, were covered with fibronectin in a similar manner than low-energy materials. But cells replaced the proteins much faster and spread much more effectively on the high-energy substrata. Low-energy substrata needed much more fibronectin adsorbed on the surface to promote cell-spreading (Grinnell, 1987). The species of adhesion protein, e.g., fibronectin, bound on the surface might attract different types of cells, such as fibroblasts, osteoblasts, and other mesenchymal cells. Therefore, the nature of the initial interface influences the kind of adhering cells. Low surface free energies of about 20-30 dynes/cm correlated with organic overlayers remaining on stearate polished metallic implants after ethylene oxide sterilization was carried out according to standard hospital procedures. The wettability of such implants was reduced, and the adhering cells were rounded without filopods *in vitro*. Scar-like lipoidal membranes developed *in vivo* and cellular adhesion was low. On the other hand, higher surface energies of about 30 to 40 dynes/cm promoted a tenacious tissue adhesion and cell-rich interfaces (Baier *et al.*, 1982). In another experiment, it was shown that around tantalum implants which were implanted for 3 weeks into the subperiosteal region of the mandible, significant differences developed between GD-treated and non-treated implants. The GD-group yielded a zone of increased cellularity on the implant surface consisting of 4-5 layers of active mesenchymal cells followed by a wider zone of lamellar fibroblastic cells (Meenaghan *et al.*, 1979). Similar results were obtained using subcutaneously implanted germanium and CoCrMo-disks for 10 and 20 days. The differences tended to disappear with increasing time of implantation (Baier *et al.*, 1984). The former studies, described above, provided some qualitative differences in the tissue reaction to implants with low versus (vs.) high surface energies. But up to now, no convincing quantitative data was available about the incorporation of sur-

face reactive GD-treated implants. Especially in a bony implantation bed, no convincing beneficial effects could be demonstrated. This might be related to long periods of implantation, to insufficient methods of investigation, e.g., removal torque, or to the implant material which was titanium in a previous study (Carlsson *et al.*, 1989).

Using histomorphometry, it was shown in former studies, that the amount of bone in contact with the interface correlates with the implant type and that this method is a valuable tool to quantitate the bone reaction to implants (Gross and Strunz, 1980; Gross and Strunz, 1985; Müller-Mai *et al.*, 1989). In a recent publication, it was demonstrated that GD-treated surface-reactive glass-ceramic implants developed higher amounts of bone in the interface, even if they are of non-bonding type (Müller-Mai *et al.*, 1992). The reason for increased bone-development is yet unknown. Therefore, the purpose of the present study was to investigate the influence of the surface conditioning GD-sterilization procedure on the incorporation of surface-reactive glass-ceramic implants in bone during the first month after implantation using light microscopy (LM), scanning electron microscopy (SEM), transmission electron microscopy (TEM), and to gain quantitative data using histomorphometry. Special emphasis was put on the ultrastructure of the interfacial healing sequence and the concomitant material response of the implant surface.

### Materials and Methods

Rectangular blocks (1.1 x 1.1 x 4 mm) of the bone-bonding glass-ceramic KG Cera (composition in weight percent: SiO<sub>2</sub> 46.2, Ca(PO<sub>3</sub>)<sub>2</sub> 25.5, Na<sub>2</sub>O 4.8, CaO 20.2, K<sub>2</sub>O 0.4, MgO 2.9) and of the non-bonding glass-ceramic KG y 213 (composition in weight percent: SiO<sub>2</sub> 38, Ca(PO<sub>3</sub>)<sub>2</sub> 13.5, Na<sub>2</sub>O 4.0, CaO 31, Al<sub>2</sub>O<sub>3</sub> 7, Ta<sub>2</sub>O<sub>5</sub> 5.5, TiO<sub>2</sub> 1) were implanted midshaft in the femur of adult male Sprague-Dawley rats weighing 350-400 grams. Prior to implantation, both implant types possessed a surface roughness of 4 µm at maximum which was produced by sawing the implant blocks. The surface of individual elevations and depressions was smooth as described in a former publication (Müller-Mai *et al.*, 1991). Both implant types were subjected to repeated ultrasonication and radio-frequency glow discharge treatment in an argon atmosphere for 2 minutes at 30 W and a pressure of 0.3 torr prior to implantation using a Harrick PDC-3XG plasma cleaner. The implants were stored in gas-free, triple-distilled water for 2 weeks to preserve the high surface energy state. Same implant materials, which were cleaned by ultrasonication, sterilized by autoclaving, and stored as described above, served as controls. Implant surface free energies were measured using different diagnostic liquids including water yielding 100 dynes/cm in the case of the GD-treated implants and 35 dynes/cm for autoclaved controls, respectively. A total of 24 implants per material was operated. The implants (n = 3 per implant-type and day for LM and histomorphometry, n = 1 for SEM, and

n = 2 for TEM) were collected 3, 7, 14 and 28 days postoperatively.

#### Light microscopy (LM)

Implant-containing femur segments were fixed for 48 hours in 5% buffered formaldehyde solution (Lillie). The specimens were subjected to a graded ethanol series (70%, 80%, 96%), each step for 24 hours followed by absolute ethanol for 2 times 24 hours. This was followed by infiltration with methylmethacrylate (MMA) for 2 to 3 days at 4°C. MMA was changed and the specimen MMA-mixture was polymerized at 40°C. The specimen containing resin blocks were orientated and were sawn perpendicular to the longitudinal axis of the implant with a sawing microtome (Leitz 1600, Leitz-Wetzlar, Germany) in approximately 70 µm thick slices. The slices were subjected to a Giemsa surface layer-staining (Gross and Strunz, 1977) or to a von Kossa/Fuchsin reaction and were embedded with Corbit. The LM-slices were subjected additionally to histomorphometric evaluation. The lengths of bone, osteoid, chondroid, and soft tissue were measured and given in per cent of the total circumference of the implant. Statistical analysis was performed using the Mann Whitney U-test using a level of significance of  $p < 0.05$  to reject the null hypothesis.

#### Scanning electron microscopy

Implants were separated mechanically from the surrounding tissue as described in detail in a previous paper (Müller-Mai *et al.*, 1990). Only the distal side of the implant remained covered with tissue. Fractures in parallel to the implant surface, opened the interface. One part of the interface represented the implant side and the other part the tissue side. The implant and the corresponding tissue were briefly rinsed in phosphate-buffered saline (PBS) solution, pH 7.2, and fixed in 4% glutaraldehyde in 0.02 M TES buffer solution, pH 7.2 for 12 hours. This was followed by washing with cacodylate buffer 0.1 M, pH 7.2 and dehydration once in 30%, 50%, 80%, and 96%, and twice in absolute ethanol for one hour each step and then dried using the critical point drying method. The dried specimens were glued onto aluminium stubs, coated with gold, and examined in a Philips SEM 505.

#### Transmission electron microscopy

The preparation for TEM started with the removal of the implant-containing femur segment in ketamin-hydrochloride/Rompun® (Bayer, Leverkusen, Germany) anaesthesia (25 mg and 5 mg/kg bodyweight, respectively) and applying intravital fixation via the abdominal aorta after injection of 10 mg Regitin® (Ciba, Wehr, Germany) for 30 seconds and 4% glutaraldehyde in cacodylate-buffer-solution, 0.1 M, pH 7.2 at 4°C. The implants were postfixed for 2 hours with glutaraldehyde as above. This was followed by rinsing with cacodylate buffer solution (0.1 M, pH 7.2) three times, 5 minutes each, and by postfixation in 1% osmium tetroxide in 0.1 M cacodylate-buffer for 1 hour in the cold. The specimens were then rinsed in veronal buffer pH 6.0 three

times (5 minutes each), stained with 0.5% uranyl acetate for 1 hour in the cold (4°C), and dehydrated in graded ethanols (70%, 80%, 90%, 96% ethanol for 15 minutes each and absolute ethanol for three times 15 minutes each). The specimens were then soaked in 1,2 propylene oxide three times for 5 minutes each, and a propylene oxide-Spurr-mixture 1:1 was used for 12 hours. Pure Spurr's low viscosity resin (Spurr, 1969) followed for 2 hours. Then, Spurr's medium was changed and the specimen-Spurr-mixture was set in gelatine-capsules, and dried in the vacuum for 2 days. The hardened specimen-containing material was glued on metal stubs and sectioned with a sawing microtome (Leitz 1600, Leitz-Wetzlar, Wetzlar, Germany) perpendicular to the longitudinal axis of the implants into approximately 500 µm thick slices. The specimens were examined by light microscopy after staining using the Richardson technique (Richardson *et al.*, 1960) to detect interface-structures of interest. The specimens were embedded again in Spurr's resin. Interesting sides at the interface were freed of resin and ceramic material first using the Leitz 1600 sawing microtome, and second using a nail-file. Only a thin layer of the glass-ceramic was left. Ultrathin sections were cut from the remaining material with a Reichert-Jung Ultracut E-microtome perpendicularly to the interface. Restaining of the sections was done with 0.5% uranyl acetate for 10 minutes at 55°C (this and all the following steps were performed at least at 55°C). The specimens were washed 3 times with double distilled water and dried on filtration paper. Lead-citrate-stain was applied for 5 minutes. At least, the specimens were washed according to the following procedure: once with 0.2 ml 10 N NaOH dissolved in 100 ml double distilled water; double distilled water; NaOH (as above) and double distilled water. The specimens were examined with a Philips TEM 410 operated at 80 kV.

## Results

#### Light microscopy, GD-implants

**KG Cera:** At 3 days after implantation, the glow-discharge treated bone-bonding implants displayed a typical blood-clot on their surfaces. In the Giemsa stained specimens, there were mainly dark-blue appearing fibers, probably fibrin, arranged in a three-dimensional network including some erythrocytes and round cells (Fig. 1). Some focal bone-contacts existed between implant corners and the compact bone of the femur.

At 7 days, most of the blood-clot was replaced by organization tissue containing many capillaries, macrophages, and rather spindle-like fibroblastic or polygonal osteoblastic cells. Macrophages were observed especially in the implant vicinity were loose implant particles were detectable. Some young trabeculae were extending from the edge of the drilling hole to the implant surface. These trabeculae were not yet fully mineralized and attached only focally to the implant surface. Histomorphometry yielded more than 12% bone-contact to the implant (Table 1).

**Table 1.** Contact length (% of the total circumference) for bone, osteoid, chondroid, and soft tissues,  $\pm$  standard error of the mean (S.E.M.) of GD-treated implants and autoclaved controls.

Material	days after implantation	Bone	Osteoid	Chondroid	Soft tissue
KG Cera GD	3	0.4 $\pm$ <1	0.8 $\pm$ <1	0 $\pm$ 0	98.8 $\pm$ <1
	7	12.5 $\pm$ 3	4.5 $\pm$ 3	0.8 $\pm$ <1	82.2 $\pm$ 4
	14	57.8 $\pm$ 12	9.2 $\pm$ 4	2.1 $\pm$ 2	30.9 $\pm$ 7
	28	92.9 $\pm$ <1*	2.7 $\pm$ <1	0.5 $\pm$ <1	3.9 $\pm$ <1
KG Cera	3	0.1 $\pm$ <1	3.5 $\pm$ 1	0 $\pm$ 0	96.4 $\pm$ 1
	7	6.4 $\pm$ 1	6.2 $\pm$ 2	0.4 $\pm$ <1	87.0 $\pm$ 2
	14	51.5 $\pm$ 3	2.9 $\pm$ <1	0 $\pm$ 0	45.6 $\pm$ 3
	28	74.2 $\pm$ 7*	10.4 $\pm$ 2	0.2 $\pm$ <1	15.2 $\pm$ 6
KG y 213 GD	3	0.4 $\pm$ <1	1.6 $\pm$ 1	0 $\pm$ 0	98.8 $\pm$ 1
	7	0.6 $\pm$ <1	4.4 $\pm$ 1	0 $\pm$ 0	95.1 $\pm$ 2
	14	3.5 $\pm$ 1	32.2 $\pm$ 11	5.8 $\pm$ 3	58.5 $\pm$ 11
	28	10.8 $\pm$ 5	30.5 $\pm$ 2	8.1 $\pm$ 5	50.6 $\pm$ 4
KG y 213	3	0.3 $\pm$ <1	3.4 $\pm$ <1	0 $\pm$ 0	96.3 $\pm$ <1
	7	1.0 $\pm$ <1	5.9 $\pm$ 1	0 $\pm$ 0	93.1 $\pm$ 1
	14	3.3 $\pm$ <1	16.5 $\pm$ 3	3.1 $\pm$ <1	77.1 $\pm$ 5
	28	7.9 $\pm$ 1	34.4 $\pm$ 5	5.4 $\pm$ 3	52.3 $\pm$ 8

\*Indicate statistically significantly different values.

**Figure 1.** GD-sterilized KG Cera implant (bottom) at 3 days after implantation covered with fibrous cell-containing tissue. Bone at the edge of the drill hole (top). LM. Bar = 100  $\mu$ m.

**Figure 2.** GD-sterilized KG Cera implant at 28 days after implantation into the femur of a rat inserted perpendicularly to the long axis of the bone. Newly formed bone trabeculae partially filling the drill hole. 100% bone-implant contact due to thin mineralized layer in areas without trabecular contact. Section in a cortical plane, distal side of the femur at left. Artificial cleft due to the sawing process. LM, von Kossa stain. Bar = 0.5 mm.

**Figure 3.** GD-sterilized KG y 213 implant at 28 days after implantation into the femur of a rat. Focal bone contacts (black) to the implant surface due to development of new trabeculae. LM. Bar = 150  $\mu$ m.

**Figure 4.** Autoclaved KG y 213 implant (I) at 28 days after implantation into the femur of a rat. Multinucleated giant cell (arrow) in contact to the implant surface in a soft tissue interface, mineralized bone (black). LM. Bar = 100  $\mu$ m.

**Figure 5.** Giant cells on the KG Cera surface, GD-treated, at 3 days after implantation. SEM. Bar = 10  $\mu$ m.

**Figure 6.** Many filopodia at the edge of a process of a giant cell interdigitate with the surface roughness produced by leaching of the glass phase in water producing a partially liberated ceramic moiety. SEM. Bar = 1  $\mu$ m.

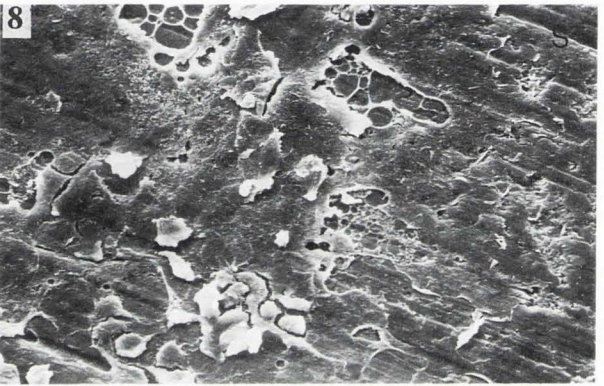
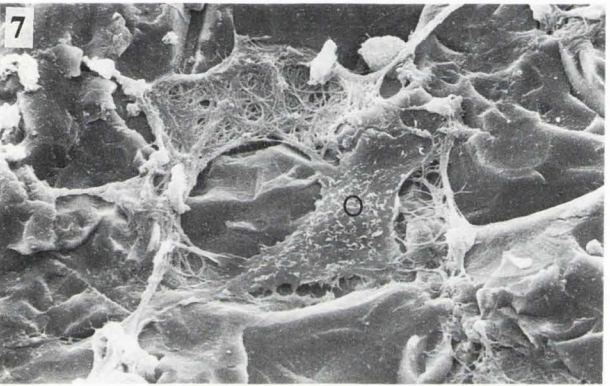
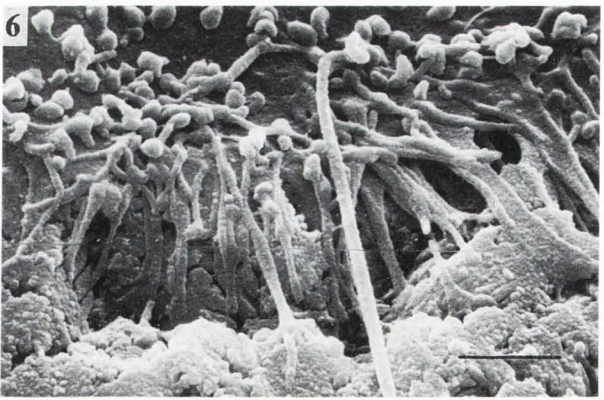
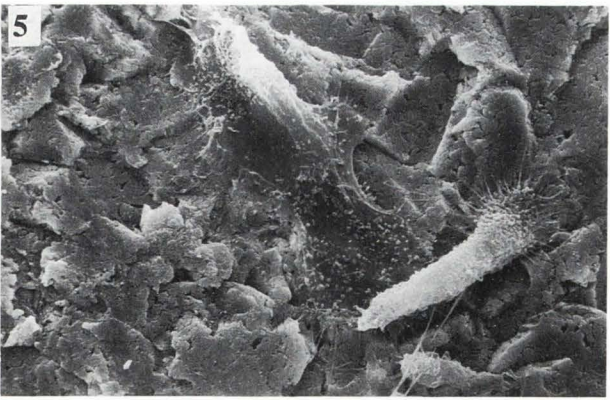
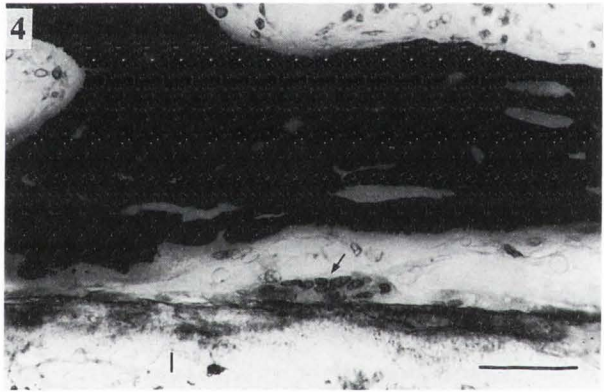
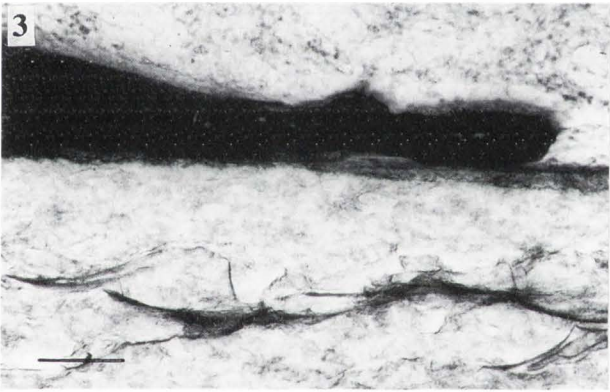
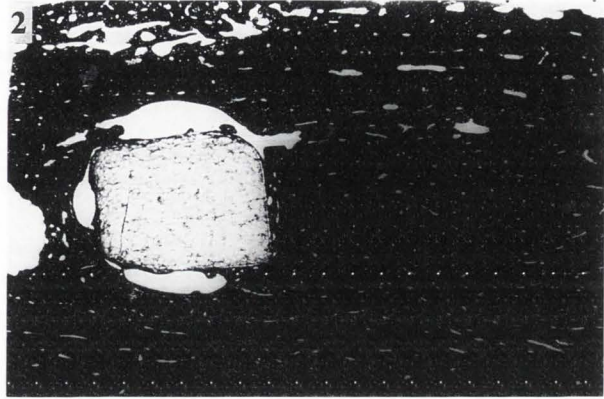
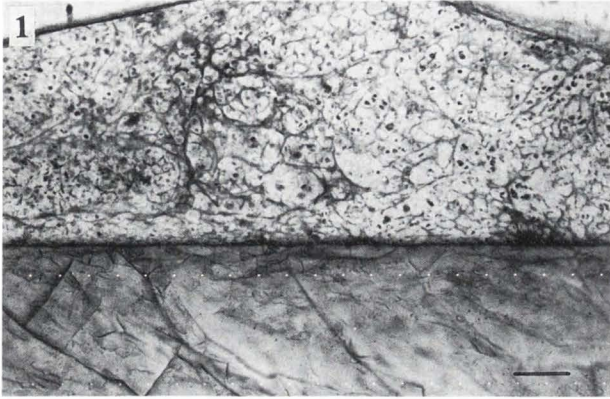
**Figure 7.** GD-sterilized KG y 213 surface at 3 days after implantation with unchanged surface morphology, attaching fibers, and an osteoblast-like appearing cell (O). SEM. Bar = 10  $\mu$ m.

**Figure 8.** Autoclaved KG y 213 implant surface at 28 days with an amorphous appearing cell-containing organic seam, probably osteoid. Implant surface without obvious morphologic changes, still with sawing marks (S). SEM. Bar = 100  $\mu$ m.

At 14 days, the situation was similar as at 7 days, except that the trabeculae were wider and attached to larger parts of the implant surface (57.8% bone-contact), forming thin bony lamellae on the implant surface between attaching trabeculae. Most of them were mineralized. Highest amounts of osteoid and chondroid were measured at 14 days (9.2% and 2.1%, respectively) indicating active formation.

At 28 days, most of the surface of the KG Cera implant was covered with new bone, either by directly inserting trabeculae or by a thin bony shell of about 20  $\mu$ m in width. One section in this group yielded 100% bone contact (Fig. 2). In average, all implants yielded significantly more bone in the interface than the control implants (92.9% vs. 74.2%, respectively, Table 1).

Glow-discharge treated glass-ceramics in bone



**KG y 213:** The glow discharge treated non-bonding implant material at 3 days showed a comparable situation as compared with the KG Cera, except that the number of cells between the fibrous fibrin-like material appeared to be higher than around the bone-bonding implant. Focal bone-contacts were due to preexisting old bone.

At 7 days, the main part of the drilling hole was occupied by capillary-rich and cell-rich organization tissue. As in KG Cera, some bone trabeculae were already formed showing a low degree of mineralization. A seam of about 20-50  $\mu\text{m}$  in width, directly on the implant surface, was free of mineralization. Bone contact was observed only occasionally when the implant corners contacted the old compact bone of the femur. Some macrophage-like cells were still detectable in the implant vicinity.

At 14 days, most of the drill hole was filled with mineralized trabeculae. An approximately 20  $\mu\text{m}$  wide non-mineralized seam surrounded the implants. This seam comprised mainly osteoid and occasionally chondroid. As in KG Cera, the highest amounts of osteoid were found at day 14 (32.2%, Table 1). Bone contact was observed when implant corners came in contact with the compact bone of the femur or at tiny mineralized areas of the implant surface within the drill hole (3.5% bone contact, Table 1).

At 28 days, most of the surface of the KG y 213 was covered with soft-tissue. Osteoid was forming a layer of approximately 10-30  $\mu\text{m}$  in width. This was interrupted by chondroid and focal bone-contacts (Fig. 3). The length of bone in the interface was 10.8% of the total implant circumference (Table 1). Osteoid and chondroid were still on the implant surface (30.5% and 8.1%) suggesting a disturbed mineralization process on KG y 213 implants as compared to KG Cera.

#### Controls, LM

**KG Cera:** In the LM, the autoclaved control group yielded a comparable healing as the glow discharge group. At 3 days, in the Giemsa-stained specimens, the bone-bonding material showed blue appearing fibers forming a three-dimensional network surrounding the implant. This tissue comprised many cells, e.g., lymphocytes, some polymorphonuclear (PMN) leukocytes, macrophages, and many erythrocytes. The fibers appeared more dense on the implant surface forming a capsule-like tissue.

7 days post-operatively, newly formed bone trabeculae filled a part of the drill-hole which were not yet fully mineralized. These trabeculae provided focal contacts with the implant surface (6.4% bone in the interface, Table 1). Between trabeculae, many productive cells and macrophages were observed.

At 14 days, a comparable histology was seen, except that more already mineralized trabeculae were observed in the drill hole. More than 51% of the interface was covered with bone and 2.9% was covered with osteoid.

28 days after implantation, 74% of the implant

was covered with bone which was significantly less than in the GD-treated implants (Table 1). There was more than 10% osteoid contact to the implant, indicating delayed mineralization as compared to GD-treated KG Cera which developed 2.7% osteoid contact at 28 days. Some lacunae were seen in the implant surface, probably produced by degradation processes. The lacunae were now covered with newly formed bone which stabilized the surface towards further degradation.

**KG y 213:** The non-bonding material KG y 213 yielded a similar histology as KG Cera, except that the number of infiltrating cells, especially PMN granulocytes, seemed to be higher.

At 7 and 14 days after implantation, a similar situation was established as described for the GD-treated implants. The amount of bone in contact to the implant surface was comparably low (Table 1). At 14 days, the amount of osteoid in the interface was significantly lower in the autoclaved control (16.5%) than in the GD-group (32.2%) indicating accelerated healing in the GD-group. In non-bonding areas, single multinucleated giant cells were observed directly on the surface.

At 28 days, the histology was similar as compared to the GD-treated implants. There was 3% less bone-contact in the control group (7.9%). Some lacunae of the implant surface were seen indicating slight degradation. At soft tissue interfaces, some multinucleated giant cells were detected as after 14 days (Fig. 4).

#### Scanning electron microscopy, GD-implants

**KG Cera:** At 3 days after implantation, after performing a fracture between implant and tissue, the surface of GD-treated bone-bonding KG Cera implants showed some areas which were covered with elongated fibroblastic or osteoblastic cells. Other just attaching cells were still roundish in shape. Between them there were single macrophage-like cells. Cells were connected by a thin film of fibers and fibrils, probably remnants of the blood-clot. Some of these fibers inserted at irregularities of the surface. Occasionally, large cells of 50  $\mu\text{m}$  and more in length were seen laying on the implant surface (Fig. 5). These cells possessed cellular processes, so-called lamellopodia with many filopods at their edges (Fig. 6). The uncovered surface of KG Cera implants showed leaching phenomena which were seen on autoclaved implants as early as 14 days after implantation (Fig. 6). This seems to be related to the GD-sterilization and subsequent storage of the implants in distilled water for 2 weeks. Due to this phenomenon the ceramic moiety of the implants was liberated partially. Leaching phenomena started at the phase transition between glass and ceramic moiety as described elsewhere (Müller-Mai *et al.*, 1991).

At 7 days post-operatively, almost the whole surface of KG Cera implants was covered with tissue. In some areas, a single layer of flat, polygonal cells covered the tissue like so-called lining cells, in other areas a lot of ECM was observed between cells indicating actively ongoing bone formation. Only single small areas

were free of cells. Some groups of cells were arranged in whirl-like or hump-like structures. Macrophages or osteoclasts were not seen. The free surface of KG Cera showed similar aspects as compared to 3 days after implantation.

At 14 days, almost the whole surface was covered with dense clusters of osteoblastic cells, some of which covered bone trabeculae which still adhered to the implant surface. Some areas between these bone trabeculae were covered with remnants of bone marrow. Other areas showed a dense film made of fibrils and fibers which were inserting at implant surface structures. Interdigitation between fibers and ceramic moiety and following mineralization might contribute to the tensile strength of the interface. A few small areas of the surface were totally free of organic material. These zones showed different degrees of leaching with partially or totally freed ceramic particles. The corresponding tissue side showed a trabecular network with bone marrow between trabeculae. Some particles of the implant surface were still in contact with the bone tissue suggesting a bone-bonding mechanism. In almost all cases, the fracture plane was either in the tissue or in the implant suggesting that the tensile strength of the interface is higher than the tensile strength of young bone or of the implant.

At 28 days post-operatively, after performing fractures in the interface level, the surface of KG Cera implants remained almost totally covered with bone tissue. Some areas of this tissue were covered with flat, polygonal cells. Other areas showed bundles of dense parallel collagen fibers at different stages of mineralization. Some osteoblasts showed stages of former differentiation as evidenced by formation of lacunae surrounded by mineralizing fibers. The intense formation of young bone tissue on the surface of KG Cera implants suggests a centrifugal bone growth starting directly on the implant surface. Only very small areas of KG Cera were not covered with tissue. The glass moiety was lost almost totally, which liberated the ceramic moiety. A dense film of fibers and fibrils was inserting at the ceramic elevations and provided a tight interdigitation between fibers and ceramic moiety. The corresponding tissue side showed trabeculae and bone marrow areas. Some trabeculae were ruptured perpendicularly to their longitudinal axis with remnants of these trabeculae still being attached to the implant surface.

**KG y 213:** The GD-treated non-bonding KG y 213 implants, at 3 days after implantation, showed a surface without obvious changes (Fig. 7). This was evidenced by saw marks on the material's surface. At higher magnification, the surface showed elevations similar to those observed for KG Cera. A large part of the surface was covered with roundish, just attaching or detaching cells. In other parts of the surface, elongated, flat, fibroblast-like cells or rather polygonal preosteoblastic cells between networks of fibers, covered the surface (Fig. 7). Between them, single macrophage-like cells with many cytoplasmic processes were seen on the surface. In a few areas, dense networks of fibrils and

fibers connected cells and implant surface.

At 7 days after implantation, most of the surface was covered with a dense layer of polygonal cells and some elongated fibroblastic cells. Few areas were free of tissue. The free surface of the implant showed no evidence of leaching phenomena. Saw marks were still detectable. No macrophages were observed on the material's surface.

At 14 days post-operatively, most of the surface was covered with a dense film of organic material. Single polygonal cells were seen on the organic material. At higher magnifications, there were still small elevations of the implant's surface with saw marks. Some circumscribed areas showed discrete signs of leaching, as evidenced by an accentuation of elevations and loosening of small implant particles indicating the onset of degradation. The corresponding tissue showed no areas of bone marrow or trabeculae. There was a film of spindle-like or polygonal cells producing a capsule-like fiber-rich tissue.

At 28 days post-operatively, parts of the surface were covered with single layers of cells or fibers. Some of these cells showed preosteoblastic phenotype with a polygonal form. Some osteoblasts were found in lacunae indicating further differentiation towards osteocytes. After performing fractures between implant and tissue single trabeculae remained on the surface of KG y 213. There was always a thin cleft between a trabeculum and the implant, suggesting that there was only bone-contact. On the whole implant surface, there was no evidence for mineralization, i.e., there were no attaching layers of collagen-fibers showing different stages of mineralization. Large cells of about 50  $\mu\text{m}$  in length and more were found attaching to the surface. These cells might correspond to the multinucleated giant cells observed in the LM. At cell-free surface areas, there were fibrillar structures, different from collagen, forming a network. The free surface exhibited few signs of leaching similar to those at fourteen days post-operatively. The surface of the corresponding tissue showed a capsule-like structure, which was partially interrupted by spaces of bone-marrow. Single trabeculae were seen in the capsule-like tissue running in parallel to the implant surface.

#### Controls, SEM

Results found in the autoclaved control materials were as described in detail in a previous paper (Müller-Mai *et al.*, 1991). It was demonstrated in that paper, that the difference of the healing occurred between the second phase (formation of granulation tissue) and third phase (formation of organ typical tissue, i.e., bone) of wound healing. This was attributed to the disturbed mineralization on the surface of the non-bonding material. In brief, at 3 days, remnants of the blood-clot covered large parts of the surface and macrophage-like cells were found settling on the surface of both of the materials. At 7 days, on the bone-bonding implants, there were polygonal cells and some rather spindle-like cells and in other parts of the surface remnants of bone trabeculae. The ceramic moiety was liberated partially on

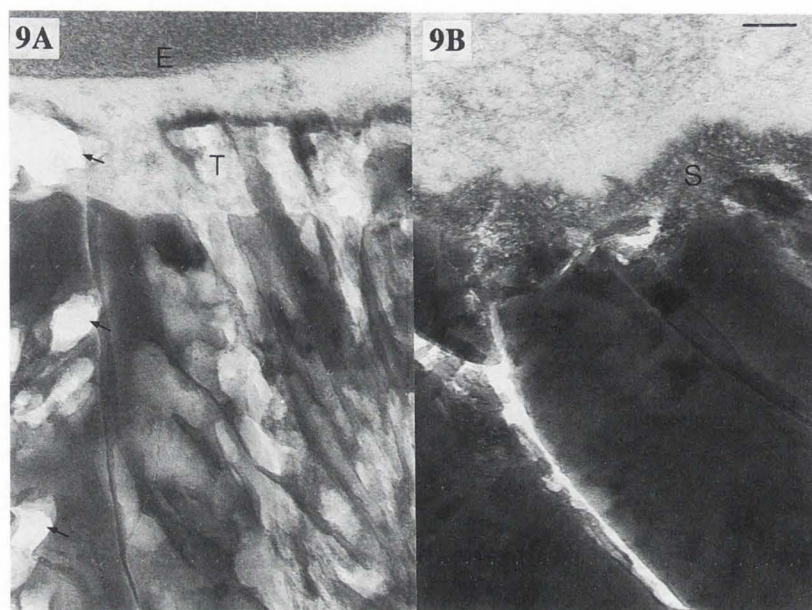


**Figure 9.** KG Cera implant surface at 3 days after implantation. **A:** GD-sterilized implant surface with an approximately  $0.1 \mu\text{m}$  wide layer showing liberated tips of the ceramic moiety (T) at the implant surface and partially liberated ceramic particles in the bulk (grey), probably due to leaching in water. Some ceramic particles were lost due to the cutting process (arrows). Thin electron-dense probably adsorbed layer covering the ceramic tips. Part of an erythrocyte (E) close to the implant surface. **B:** Autoclaved surface covered with a mineralized appearing seam (S) of about  $0.1 \mu\text{m}$  in width. Ceramic moiety totally covered by the glass moiety (black). TEM. Bar =  $0.1 \mu\text{m}$ .

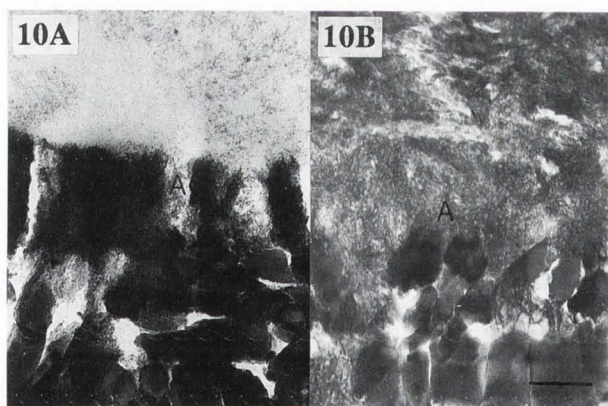


**Figure 10.** GD-treated KG Cera implant surface at 7 days after implantation. **A:** Thin amorphous appearing seam (A) of approximately  $0.3 \mu\text{m}$  in width on the implant surface in a non-bonding area, probably due to the development of a Ca/P-rich layer on the implant surface. **B:** Amorphous, probably afibrillar, approximately  $0.3 \mu\text{m}$  wide Ca/P-rich layer (A) in a bone-bonding area. TEM. Bar =  $0.2 \mu\text{m}$ .

the implant surface. At 14 and 28 days, the histology was similar to that at 7 days, but the amount of still adhering bone trabeculae increased. At 28 days, most of KG Cera's surface was covered with trabeculae and bone-marrow. On the other hand, at 7 days, the non-bonding material still showed macrophage-like cells on the surface. There were no signs of bone-formation and little tissue-contact. At 14 and 28 days, the surface displayed less cells but still, there were no signs of bone formation. There was just a film of organic material containing some cells in some parts of the implant surface (Fig. 8). The implant surfaces showed similar as-

pects as described for GD-treated implants with liberated ceramic particles in the KG Cera and only very little changes in the KG  $\gamma$  213.

#### Transmission electron microscopy, GD-implants

**KG Cera:** At 3 days after insertion some parts of the surface of the GD-sterilized KG Cera implants were covered with a layer of electron-dense fibrous material which seemed to consist in part of the fibrin of the blood-clot. This layer had an average width of  $2 \mu\text{m}$ . Most of the fibers ran parallel to the implant surface. In this layer, some inflammatory cells, mainly PMN leukocytes and macrophages, single mast cells, and erythrocytes were observed. Most of the cells showed intracytoplasmic vacuoles, lipid droplets, and swollen cell organelles. Remnants of cell organelles were seen free in between the electron-dense fibers. In other parts, the surface was covered with electrolucent ECM, sometimes containing vesicular structures. The surface of the glass-ceramic showed obvious signs of leaching. Directly on the surface, the structure of the material changed showing star-like structures of about  $0.7 \mu\text{m}$  in diameter or an approximately  $0.1 \mu\text{m}$  wide zone, in which the glass moiety was removed totally. Tips of the ceramic moiety were liberated contributing to the higher rugosity as compared to the control implants at this time (Fig. 9A, 9B). Such particles were not visible in the bulk, being still covered with the glass-moiety. On top of the ceramic tips, a thin, approximately  $0.01 \mu\text{m}$  wide electron-dense layer was seen, which differed in structure and stainability as compared to the mineralized seam of the KG Cera control implants.

At 7 days, some parts of the implant surface were covered with a 1-2  $\mu\text{m}$  thick leaching zone showing the same morphology as described at 3 days. The leaching zone was covered with 2-3 layers of elongated productive cells. Cellular membranes came in direct contact

with the material or were separated from the implant by electron-dense fibrous material or by a rather electro-lucent granular material. In some areas, interfacial cells possessed microvilli on their cellular membranes towards the tissue side. Single erythrocytes or infiltrating cells, e.g., macrophages, were seen between the elongated interfacial cells. Some areas of the implant surface were covered by a thin, amorphous appearing seam of less than  $0.5\ \mu\text{m}$  in width (Fig. 10A) or by a similar appearing seam and mineralized collagen-rich ECM (Fig. 10B). Occasionally, matrix vesicles were observed close to such seams (Fig. 11). Osteoclastic cells were still observed on the implant surface. Some particular material seemed to loose contact to the bulk below the osteoclastic cell membrane (Fig. 12). The next layers towards the edge of the drill hole consisted of partially mineralized ECM and osteoblastic cells. Between already mineralized material and osteoblastic cells, many matrix vesicles were seen in a collagen-rich ECM indicating actively ongoing calcification. Capillaries were observed in this layer. Between the layer of osteoblastic cells and the compact bone of the drill hole, a network of fine ECM was detectable. This layer consisted of many fine fibrillar structures, probably hyaluronic acid, and proteoglycan granules between large macrophage-like cells. This zone was separated from the mineralized old bone of the femur by lining cells and a collagen-rich ECM.

At 14 days, some parts showed bone-bonding. In other parts, elongated cells were seen in the interface. The cells were separated from the implant surface by a small seam of fine fibrillar and fine granular material. Occasionally, extracellular matrix vesicles were observed in this zone. Some cells died at the interface as indicated by intracytoplasmic vacuoles, lipid droplets, and condensation of cytoplasmic structures. The next zone towards the tissue side comprised of approximately 5 layers of flattened or cuboidal cells. The cells were embedded in a collagen-rich ECM. Osteoblastic cells were seen between this zone and the collagen-rich ECM covering the old bone of the drill hole. In this zone, some capillaries were seen. The implant surface showed different aspects. In non-bonding areas, some interfacial segments had a liberated ceramic moiety as described above. This zone had a width of at least  $1.2\ \mu\text{m}$  (Fig. 13). In other areas, there was a dense amorphous zone of the implant material directly in contact with the tissue of approximately  $0.2\text{--}0.4\ \mu\text{m}$  width covering the bulk material similar to that described at 7 days. This zone might correspond to the carbonated hydroxyapatite layer (Neo *et al.*, 1992a,b) which develops on the Ca/P-rich layer and the Si-layer typical for bonding glasses and glass-ceramics (Hench *et al.*, 1977; Kitsugi *et al.*, 1987b). In bone bonding areas, a similar seam in width and morphology was observed linking the bulk material and mineralized collagen (Fig. 10B).

At 28 days, most of the TEM-sections showed bone-bonding interfaces. In non-bonding areas the interface was mostly covered with a thin electron dense, non-mineralized seam ( $0.05\text{--}2\ \mu\text{m}$  wide) which seemed to

consist of remnants of died cells. Similar spots were found in the collagen-rich ECM which was not in contact with the implant showing the same morphology. In other non-bonding parts of the interface, a collagen-rich ECM was seen, some already mineralized foci indicated active calcification. The collagen was mostly running in parallel to the implant surface. The ECM contained a lot of extracellular matrix vesicles, some chondrocyte-like cells sometimes arranged in groups, which were surrounded by a thin seam of non-collagenous ECM which in turn was surrounded by the mineralizing collagen-rich ECM. All stages of cells, ranging from living chondrocyte-like cells to electron-dense condensed remnants of these cells, were found in the matrix and directly on the implant surface. Many vesicular structures, obviously originating from these degenerating cells, and similar to matrix vesicles, were found surrounding and within the electron-dense cell-fragments. Some of these vesicular structures were partially calcified and seemed to act in a comparable manner to matrix vesicles. The material's surface showed cross-cut ceramic particles of about  $0.7\ \mu\text{m}$  in diameter. Between glass-ceramic surface and mineralized surface, there was a rather homogenous, amorphous seam of  $0.2\text{--}0.4\ \mu\text{m}$  in width linking tissue and implant as described at 14 days.

**KG y 213:** At 3 days, the GD-treated non-bonding material was covered with constituents of the blood-clot, comprising inflammatory cells such as PMN leukocytes and macrophages, many erythrocytes, and electron-dense fibrin-like material. A  $2\text{--}4\ \mu\text{m}$  wide layer of this fibrous fibrin-like material covered the surface of the material (Fig. 14). This material contained irregularly shaped vesicular structures, probably remnants of dead cells. In some areas of the interface, the electron-dense fibrin-like material was separated from the implant by a zone less than  $1\ \mu\text{m}$  wide, consisting of fine fibrillar and granular structures. Cells were also sometimes separated from the material by this layer. Most inflammatory cells were vacuolized, and possessed intracytoplasmic lipid droplets and residual bodies indicating cell death. At higher magnification, probably an adsorbed seam of electron-dense material was observed on the implant surface which was less than  $0.1\ \mu\text{m}$  wide. The implant material showed no density differences indicating that the amount of leaching seems to be lower as compared to the KG Cera.

At 7 days, a part of the interface of the non-bonding material was covered with an electron-dense fibrous layer of approximately  $1\ \mu\text{m}$  width, or in other parts, with elongated cells, some erythrocytes and some infiltrating cells, especially macrophages and PMN leukocytes. The electron-dense fibrous material was sometimes separated by an electro-lucent granular material of  $0.2\ \mu\text{m}$  thickness. Cell-covered parts of the interface showed remnants of the blood-clot, especially macrophages with dense cytoplasm, many mitochondria, and lamellopodia on their plasma-membranes. The plasma-membranes of these cells were in direct contact with the implant surface. Some of these cells contained small

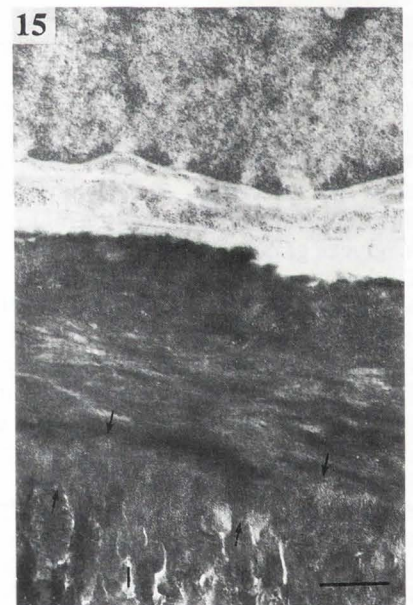
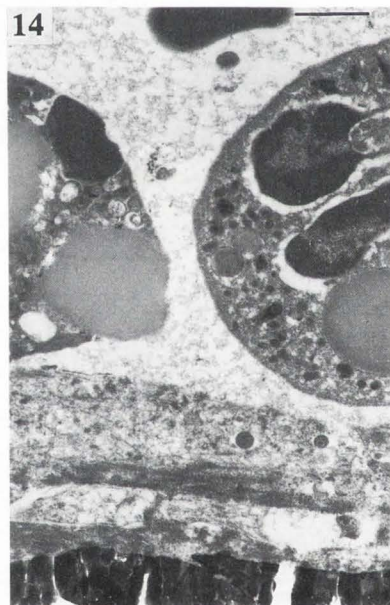
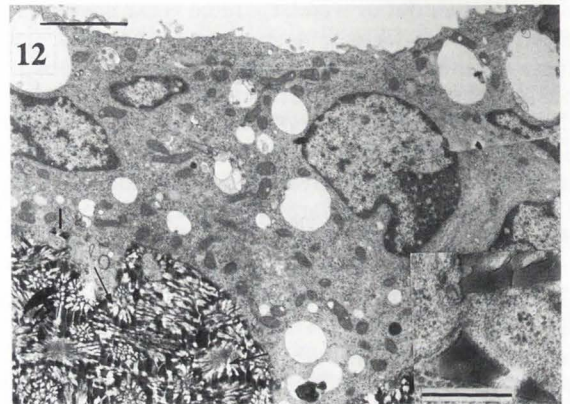
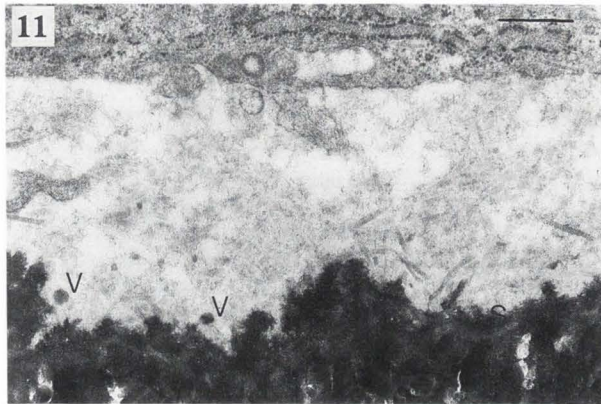


**Figure 11.** GD-treated KG Cera implant surface (black, bottom) at 7 days after implantation covered with a mineralized seam (S) due to bone-bonding in the vicinity of a productive cell (top) and collagen-rich extracellular matrix (middle) containing crystal matrix vesicles (V). TEM. Bar = 0.5  $\mu\text{m}$ .

**Figure 12.** GD-treated KG Cera implant surface at 7 days after implantation. Multinucleated giant cell in direct contact to the implant surface with incorporated particles of implant origin (I). Implant appears microporous due to leaching in water prior to implantation. Pores (arrows) at the phase transition between glass-phase (black) and ceramic moiety (grey). Inset: Higher magnification of one part of the giant cell with incorporated particles of implant origin. TEM. Bar = 2  $\mu\text{m}$ ; inset, bar = 0.4  $\mu\text{m}$ .

**Figure 13.** GD-treated KG Cera implant surface at 14 days after implantation. Leaching zone in non-bonding area with totally liberated ceramic particles. TEM. Bar = 0.5  $\mu\text{m}$ .

**Figure 14.** GD-treated KG y 213 implant surface at 3 days after implantation, covered with fibrous material of the blood-clot and remnants of polymorphonuclear leukocytes. Some vesicular structures in the fibrous material close to the interface. TEM. Bar = 1  $\mu\text{m}$ .

**Figure 15.** GD-treated KG y 213 implant surface (I) at 28 days after implantation with bone-bonding via an afibrillar appearing, probably Ca/P-rich layer (arrows) in the vicinity of a cell (top). TEM. Bar = 0.5  $\mu\text{m}$ .

particles of implant origin. The next layer consisted of approximately 4 layers of spindle-like fibroblastic cells. Between the cells, some non-cross-banded fibrils were seen. This layer was followed by a zone of collagen-rich ECM containing osteoblastic cells, capillaries, and matrix vesicles. In between, some macrophages, phagocytosing remnants of dead cells, were sometimes seen. The next layer was old fully mineralized bone. The implant surface showed no obvious changes.

At 14 days, most parts of the implant surface were covered with either mineralized tissue or 2-3 layers of osteoblastic and elongated cells. Some cells contacted the implant surface via slim short cytoplasmic processes. A fine granular material was present between the cellular plasma membrane and the implant surface. This material separated the cellular plasma membrane and the implant surface. In other parts, plasma membranal parts contacted the implant surface directly. The cells in contact with the material showed intracytoplasmic vacuoles and a few single lipid droplets indicating cellular degeneration. Cells without direct contact were rather productive, as indicated by widened endoplasmic reticulum. In a few interface areas, a 0.5  $\mu\text{m}$  wide electron-dense seam, as described above, was observed. Directly on this seam, mineralization of collagen-rich ECM started. Matrix vesicles were seen in such areas. The second layer consisted of osteoblastic cells, single macrophages, and erythrocytes. This layer contained several capillaries. In between the cells, there were some remnants of the fibrous fibrin-like material, and occasionally islands of already mineralized material and collagen containing a few matrix vesicles indicating little mineralizing activity. Lining cells sealed off this zone against the osteoid matrix of the dense, old, fully mineralized bone. The material surface showed the same aspects as described before.

At 28 days, the surface was either covered with a 0.5  $\mu\text{m}$  wide electron-dense seam as described before or with cells, remnants of cells which were in part separated from the surface by a thin seam of ECM, or a collagen-rich ECM. Some cellular processes extended into clefts of the material. Some of these cells were of chondrocyte-like type and single chondrocyte-like cells died before. The surface of the material was smooth and showed no obvious signs of degradation. In some parts of the surface, roundish defects, with diameters of approximately 0.05  $\mu\text{m}$ , were seen. Single foci with bone contact were detected, sometimes in a layer of 1-4  $\mu\text{m}$  in width (Fig. 15). This zone was followed by collagen-rich ECM, then in turn, productive cells and some dying cells were observed, followed by a cell-rich zone with single eosinophilic cells, mast cells, PMN leukocytes, and many macrophages which showed a lot of loose implant particles in their cytoplasm or in the surrounding ECM. The next layers consisted of lining cells, collagen-rich ECM, and the mineralized bone of the drill hole.

#### Controls, TEM

**KG Cera:** At 3 days, the bone-bonding implants

were totally covered with fibers and cells of the blood-clot, i.e., leukocytes, many macrophages and erythrocytes. Some macrophages seemed to phagocytose parts of the fibrous material of the blood-clot as well as remnants of dead cells. Some productive cells were already observed invading the blood-clot. The implant surface was still free of such cells. Infiltrating cells with cell membranes in direct contact with the implant surface showed intracytoplasmic vacuoles and lipid droplets. Most areas of the interface were covered with an electron-dense mineralized appearing seam of about 0.1  $\mu\text{m}$  width (Fig. 9B). Focally, roundish nodules similar in structure protruded into the tissue. Some spots of already mineralized material were found on the implant surface and in the ECM nearby.

At 7 days after implantation, KG Cera showed areas of the glass-ceramic surface which were covered with an electrolucent fiber-containing material, probably ground substance. Some fibers within this material were cross-banded, which is typical for collagen, and ran parallel to the interface. At other areas of the surface of KG Cera, there was a 0.05-1  $\mu\text{m}$  wide electron-dense seam. Occasionally, this seam contained some needle-like crystals of about 0.03  $\mu\text{m}$  in length, probably hydroxyapatite. At some places, these crystals formed a thin layer on the material's surface. Osteoblasts were in the vicinity of the implants, mostly separated from the implant by a small seam of ground substance. Some cellular membranes were in direct contact to the implant surface. These cells were orientated with their longitudinal axis in a parallel manner to the implant surface. Some of the osteoblasts showed intracytoplasmic vacuoles in contact with the cellular membrane during release of an amorphous material into the gap between cell membrane and material's surface. Between osteoblasts, there were macrophages, sometimes containing phagocytosed particles of the glass ceramic and phagocytosed remnants of organic material, e.g., erythrocytes. The second layer towards the tissue side consisted of approximately 4 layers of elongated cells which were mostly non-active. The third layer comprised active osteoblastic cells and some interspersed macrophages within a collagen-rich ECM containing a large amount of matrix vesicles and calcified globules. The surface of the glass ceramic was mainly homogeneous, i.e., the crystalline and the amorphous glass moiety was preserved. Only in small areas, there were small pores suggesting degradation of the implant. At these areas there was no electron dense seam and there were no hydroxyapatite crystals. Some of these pores contained processes of macrophages.

At 14 days post-operatively, the seam connecting the implant with mineralized tissue as described at 7 days was present. At other areas, there was a tight connection between implant and already mineralized tissue. Next to the mineralization zone there were osteoblasts, endothelial cells of young vessels and macrophages. Some macrophages and occasionally some osteoblastic cells contained tiny black particles of implant origin.

Between the mineralizing zone on the implant and osteoblasts, there were matrix vesicles suggesting a proceeding mineralization. This suggests a centrifugal mineralization, i.e., a centrifugal process which starts on the implant surface. Non-bonding areas consisted mainly of cell rich soft-tissue with many macrophages, and some other round cells such as PMN leukocytes, some chondrocyte-like cells, but also foci of collagenous ECM contacted the implant surface. The next layer consisted of osteoblasts, followed by collagen-rich ECM, and mineralized bone. Some macrophages were seen directly on the implant surface, some of which contained phagocytosed implant particles.

At 28 days, bone-bonding areas were almost exclusively seen. If there was soft tissue close to the interface, it was mostly separated from the surface by a few  $\mu\text{m}$  wide mineralized seam sometimes containing osteocytes. The osteoblast-covered mineralized tissue separated the implant and the bone marrow. In the bone marrow, some macrophages were detected containing incorporated implant particles. Single cells in contact to the surface were large macrophage-like cells with a vacuolized cytoplasm or chondrocyte-like cells. Such surface areas showed obvious signs of degradation. In such areas, there were no osteoblasts or matrix vesicles.

**KG y 213:** At 3 days, the non-bonding implants were covered with fibers of the blood-clot. Single macrophages were detected in this layer on the implant surface. Some contained incorporated particles of implant origin. Between electron-dense fibers, there were PMN leukocytes, round cells, and erythrocytes. Cells in contact with the implant surface showed intracytoplasmic vacuoles. As compared to the GD-treated implants, the material covering the implants contained less cells.

At 7 days after implantation the non-bonding glass-ceramic KG y 213 showed no signs of leaching or degradation. The main part of the interface was covered with a rather electrolucent granular ground substance, in some foci containing cross-banded fibers. These fibers ran parallel to the interface. Occasionally, there were remnants of blood, erythrocytes and organelles of disintegrated cells in the interface. The implant surface showed small gaps with a width of 0.1-0.15  $\mu\text{m}$  which were filled with a fine granular material, probably remnants of interstitial fluid. There were some larger gaps, probably due to fractures during the sawing process, which were filled with the same granular material, with ground substance, and with cell processes. Some osteoblastic and fibroblastic cells were evident, aligned parallel with their longitudinal axis directly on the material's surface. These layers on the implant surface were encased by approximately 15 layers of elongated cells. In between these cells, sometimes there was an electron-dense fibrous material, probably remnants of dead cells of the former blood-clot. The cells at the interface contained organelles with an amorphous substance in their cytoplasm and some of them were producing collagen. Between them, there were some macrophages occasionally containing phagocytosed implant particles. Seldom,

there were some matrix vesicles with the typical trilaminar membrane in the ground-substance near the interface. These matrix vesicles were never in direct contact with the surface. Additionally, there was no contact of the non-bonding material KG y 213 to mineralized tissue at 7 days after implantation in the TEM sections.

At 14 days, there were mainly ground-substance with cross-banded fibers, some osteoblasts, and some spindle-like fibroblastic cells or macrophages observed in the interface. In one area, there were endothelial cells of a newly formed vessel directly at the surface of KG y 213 (Fig. 16). Sometimes, there was a tiny gap between the cellular membrane and the material surface filled with electrolucent material. In other parts, cellular membranes were in direct contact to the implant surface. In contrast to the bone bonding material KG Cera, mineralized tissue followed after some layers of concentric cells. At 14 days after implantation, there were no signs of leaching or degradation of the surface. Small gaps of the surface were filled with a fine-granular material comparable to the material at 7 days.

At 28 days, most of the surface was covered with a collagen-rich ECM. Within the ECM, there were single osteoblastic cells, matrix vesicles, and some chondrocyte-like cells. Osteoblasts showed widened rough endoplasmic reticulum, indicating a productive stage. Chondrocyte-like cells showed all stages from living cells to degenerating dying cells (Fig. 17). Some scattered vesicular structures were seen, some containing crystalline material. Some areas of the implant surface were covered with an electron-dense layer of about 0.2  $\mu\text{m}$  width (Fig. 18). The surface of the material still showed no obvious signs of leaching. But particles of implant origin were detected incorporated in macrophages, indicating partial degradation (Fig. 19). The pores within the material were filled with an electrolucent granular material, probably remnants of extracellular fluid.

## Discussion

It was demonstrated in this study that the tissue reaction to surface-reactive glass-ceramic implants can be influenced by changing physical and chemical surface properties. These processes, leading to an improved incorporation, are not yet fully understood. In the LM, the typical healing sequence which was described in former studies was observed (Gross and Strunz, 1980, 1985). There was no obvious difference between the GD-treated implants and autoclaved controls except for the higher amount of bone in the interface, an earlier osteoid development with a maximum at 14 days, and more chondroid even in the non-bonding GD-group. Due to the low resolution, LM-results did not provide a sufficient explanation for the higher amount of bone. Therefore, SEM and TEM of the interface were applied demonstrating differences in both, the material and host response. The differences in the host response seemed to depend on different surface free energy states of the implants and/or to following storage in distilled water

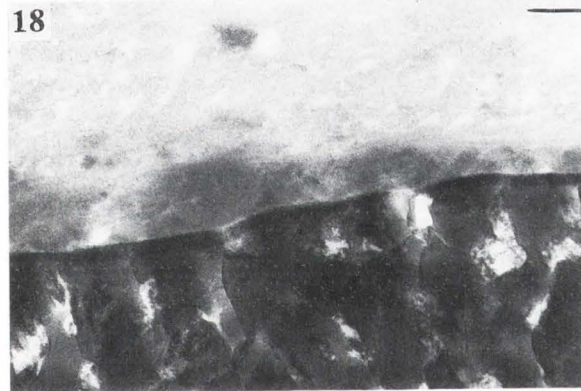


**Figure 16.** Interface of an autoclaved KG y 213 implant (black, bottom) at 14 days after implantation with a blood vessel in direct contact to the implant surface. Some endothelial cells with phagocytosed implant material (arrows). TEM. Bar = 5  $\mu\text{m}$ .

**Figure 18.** Adsorbed electron-dense film covering a KG y 213 implant surface at 28 days. TEM. Bar = 0.2  $\mu\text{m}$ .

**Figure 19.** Tissue in the vicinity of a GD-treated KG y 213 implant at 28 days after implantation showing a macrophage-like cell with many incorporated particles of implant origin. TEM. Bar = 1  $\mu\text{m}$ .

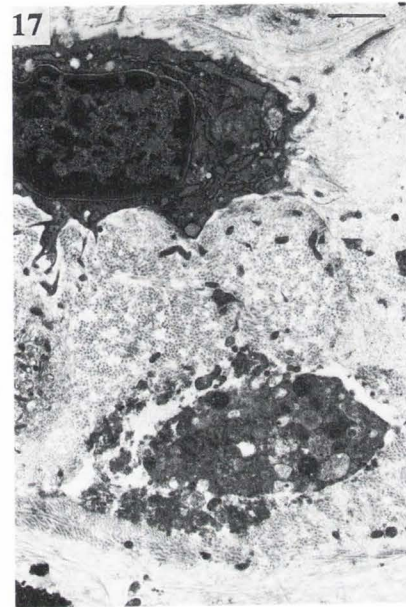


**Figure 17.** Cell remnants and collagen-rich ECM in the vicinity of a KG y 213 implant at 28 days. TEM. Bar = 1  $\mu\text{m}$ .

leading to different material responses which in turn seemed to influence the host response. GD-treatment is known to alter the outermost surface properties of implants, e.g., in a polymer the molecular composition of the outermost 3 nm was changed by oxidative etching processes which led to increased  $\text{N}_2$  and  $\text{O}_2$  amounts (Pratt *et al.*, 1989). Similar processes act on glass-ceramics in removing all of the organic contaminants but probably with minor influence on the chemical surface composition. On one hand, this is due to the higher energetic bonds in such materials, and on the other hand, it is related to the GD-process which was carried out here in an argon atmosphere. A probable chemical difference between GD-treated implants and autoclaved controls might be produced by storage in water prior to implantation. It is assumed that the rate of leached implant ions was higher in the GD-group since the protective contamination layer of organic and inorganic contaminants usually occurring on the surface was removed. Storage in water led to a leached zone on the surface of the GD-treated bone-bonding implants and to a seam probably consisting of Ca/P-compounds on the autoclaved implants. Such electron-dense seams are well-known to develop on surface-reactive bone-bonding implants. In the case of hydroxyapatite, such seams were observed and consisted of carbonated hydroxyapatite (Daculsi *et al.*, 1990; Jarcho, 1981; Orly *et al.*, 1989). In the case of glasses and glass-ceramics, Si-rich and Ca/P-rich interlayers provide a chemical bonding of the implant to bone (Andersson and Karlsson, 1991; Hensch *et al.*, 1977; Kitsugi *et al.*, 1987b; Ohtsuki *et al.*, 1991). Such interfacial layers also develop in various

fluids *in vitro* (Andersson and Kangasniemi, 1991) and after intraperitoneal implantation (Pernot *et al.*, 1985) and are able to produce chemical bonding even between two blocks of such an implant material (Kitsugi *et al.*, 1987a). Similar reactions were also observed in other studies using different Ca/P-ceramic tooth implants in humans. Calcium oxide and even dense hydroxyapatite implants showed higher dissolution rates *in vitro* when being GD-sterilized as compared to autoclaved controls. In additional *in vivo* experiments, the GD-group yielded resistance against rotational force at 4 weeks, whereas, sterile implants provided directly from the manufacturer, needed 3 months, thus the GD-treatment leads to faster immobility of loaded bone-bonding implants (Sendax and Baier, 1992). These results point to the solubility of the implant surface which might differ in GD-treated and autoclaved glass-ceramic implants and might explain why other investigators did not measure significant differences. Those studies used titanium implants for periods of up to 7 weeks. In addition to the different implant material, the time of investigation seemed to be too long, so that possible differences were not detected even if the implants were inserted in temporary bone ischaemia to prevent adsorption of blood-constituents to the implant surface (Carlsson *et al.*, 1989, Wennerberg *et al.*, 1991).

Cell attachment, adhesion, and spreading on artificial substrata depends, among other possibilities, on the chemical and physical nature of the substrate. Under *in vivo* conditions, in cases of high surface energy associated with hydrophilic properties and a better wettability, first contact between implant and host tissue should be provided by adsorbed serum proteins. This might explain, in part, the electron-dense layer directly on the implant surface of GD-treated specimens at 3 and 7 days observed in the TEM. This layer seemed to originate partially from dead cells which colonized the implant surface prior to cell death. Their remnants might have been adsorbed after cell death onto the implant surface and contributed to the production of the dense condensed film. A similar layer was described in an earlier publication using metal implants subcutaneously. Implant surfaces were covered with a protein dominated "conditioning" layer on which active fibroblasts were observed (Baier *et al.*, 1984). Between remnants of dead cells, a lot of membrane-bound vesicular structures were detected which were interpreted to originate from these cells. The number of dying cells in the interface seemed to be higher on GD-treated surfaces. At 3 and 7 days this was related to death of leukocytes, at 14 and 28 days, a higher amount of chondroid developed (Table 1) and many of the chondrocyte-like cells degenerated especially on GD-treated implant surfaces, thus producing vesicular structures in the electron-dense layer at the implant surface. Such vesicles might contribute to the mineralization as initial foci of crystal formation similar to matrix vesicles. This might contribute to higher rates of bone-contact to GD-treated implants. Vesicular structures as described above, produced by all of these differ-

ent cell-types, might additionally serve in initiating primary crystal formation. This interpretation is corroborated by former studies since similar processes were also described in electron microscopic studies of ectopic calcification of the human aortic valve and aortic media. Calcification was associated with accumulated lipids and vesicular structures, both being obviously cellular degradation products (Kim, 1976). In aging hyaline cartilage, vesicular remnants of cells acted as primary foci of hydroxyapatite crystal-formation which was explained by calcium-binding properties of such structures (Bonucci and Dearden, 1976). A former *in vitro* study provided additional support for this hypothesis. Synthetic multilamellar, multicompartamental vesicular structures, so-called liposomes, induced intraluminal Ca/P-precipitation at the inner part of their membranes leading to clusters of intraliposomal apatite mineral (Heywood and Eanes, 1987).

In the SEM and TEM, more osteoclast-like cells were detected at 3 and 7 days on the surface of the GD-KG Cera-group as compared to the control. These cells seemed to contribute to implant degradation since the cells were able to phagocytose implant particles. Typical ruffled borders were not observed in the TEM. But the cells shared other features with osteoclasts. There was a polarity of the cells with microvilli at the dorsal cellular membrane. The cytoplasm contained a lot of mitochondria, perinuclear golgi complexes, and rough endoplasmic reticulum in the basal portion of the cell. Large extracellular recesses, which are also thought to be typical for osteoclasts, are demonstrated in the cell in Fig. 12. Zones resembling the so-called clear zones were detected. In the SEM, cellular processes with many filopods were detected (Figs. 5 and 6). It was shown in former publications that when resorption of osteoclasts has stopped and the cells start to migrate, the edges of such formerly resorptive zones, i.e., ruffled borders, can be demonstrated within newly formed resorption lacunae (Chambers *et al.*, 1984; Müller-Mai *et al.*, 1990). Therefore, the cells might be able to seal up the area underneath their cellular membranes and might lower the pH in this region leading to increased solubility of this implant surface area. This in turn might contribute to the liberation of particles which were phagocytosed by the osteoclast-like cells as demonstrated in Fig. 12. The reason for the presence of such cells on the GD-treated KG Cera is not yet clear. Possible factors contributing to an attraction of osteoclasts could be the formation of chemical compounds on the implant surface due to storage in water which are attractive for this cell type. Physical properties also seem to influence the colonization of the implant surface with different cell-types. This suggestion might be supported by the fact that osteoclast-like cells were detected on the surface of GD-treated KG Cera implants which possessed a higher rugosity of the implant surface created by leaching processes in water. It was shown in former studies, that macrophages and osteoclasts are more common on surfaces with higher rugosity (Brunette, 1988; Gomi *et al.*,

1992; Rich and Harris, 1981). No osteoclast-like cells were observed on autoclaved KG Cera implants and on the KG y 213 specimens at 3 and 7 days. In the TEM sections, the KG y 213 material neither showed signs of leaching nor increased rugosity, but adsorption of an electron-dense film of organic material.

In the present study, there seemed to be lower numbers of macrophages on GD-materials. The occurrence of macrophages on both of the surfaces in different numbers, i.e., on autoclaved and GD-treated materials, corresponds to a former study using the same, but autoclaved implant materials. Macrophages disappeared at approximately 7 days in the case of the bone-bonding material concomitant to beginning mineralization of the implant surface (Müller-Mai *et al.*, 1991). Since the amount of bone in the interface of GD-treated implants was higher, this process might contribute to the decrease of the macrophage numbers. Additionally, a former study using macrophages *in vitro* showed that macrophages settled on hydrophobic substrata whereas fibroblasts preferred hydrophilic substrata (Rich and Harris, 1981). Since GD-treatment is known to increase the surface wettability and many productive mesenchymal cells were detected on the GD-treated implant surfaces, the results obtained here are in accordance with the former *in vitro* findings.

In conclusion, GD-treated surface-reactive bone-bonding and non-bonding implants showed significant differences as compared to autoclaved controls. This ultrastructural investigation might explain, in part, the higher bone formation-rate in contact to GD-treated surfaces. This seems to be related to a different rate of leaching which has to be proven in controlled *in vitro* leaching experiments. The total removal of the protective contamination layer on the GD-treated implant surfaces seems to allow a higher elution-rate of implant constituents from the implant surface. This, in turn, produces a rugosity by liberation of the ceramic moiety of the KG Cera implants at 3 days which might additionally contribute to a high leaching rate because of the higher surface area and therefore, to a higher alkalinity of the interface. In addition, forming cells dominated on GD-sterilized surfaces. Osteoclast-like cells seemed to contribute in part to implant degradation and did not disturb the implant incorporation significantly. The number of macrophages was reduced. Membranous parts of dying cells especially on GD-treated surfaces could have provided additional foci of primary crystal formation. Thus, the GD-treatment seems to be suitable at least for sterilization of surface-reactive implants to reduce the time to establish functionality of implants and to minimize possible degradation processes.

### References

- Andersson ÖH, Karlsson KH (1991) On the bioactivity of silicate glass. *J. Non-Cryst. Solids* **129**, 145-151.  
 Andersson ÖH, Kangasniemi I (1991) Calcium

phosphate formation at the surface of bioactive glass *in vitro*. *J. Biomed. Mater. Res.* **25**, 1019-1030.

Baier RE (1982) Conditioning surfaces to suit the biomedical environment: Recent progress. *J. Biomech. Eng.* **104**, 257-271.

Baier RE, Depalma VA, Furuse A, Gott VL, Kammlott GW, Lucas T, Sawyer PN, Srinivasan S, Stanczewski B (1975) Thromboresistance of glass after glow discharge treatment in argon. *J. Biomed. Mater. Res.* **9**, 547-560.

Baier RE, Meyer AE, Akers CK, Natiella JR, Meenaghan M, Carter JM (1982) Degradative effects of conventional steam sterilization on biomaterial surfaces. *Biomaterials* **3**, 241-245.

Baier RE, Meyer AE, Natiella JR, Natiella RR, Carter JM (1984) Surface properties determine bioadhesive outcomes: Methods and results. *J. Biomed. Mater. Res.* **18**, 337-355.

Baier RE, Natiella JR, Meyer AE, Carter JM, Fornalik MS, Turnbull T (1986) Surface phenomena in *in vivo* environments. In: *Materials Sciences and Implant Orthopedic Surgery*, Kossowsky R, Kossovsky N (eds.), Martinus Nijhoff Publishers, Dordrecht, The Netherlands, pp 153-188.

Bonucci E, Dearden LC (1976) Matrix vesicles in aging cartilage. *Federation Proc.* **35**, 163-168.

Brunette DM (1988) The effect of implant surface topography on the behaviour of cells. *Int. J. Oral Maxillofac. Implants* **3**, 231-246.

Carlsson LV, Albrektsson T, Berman C (1989) Bone response to plasma-cleaned titanium implants. *Int. J. Oral Maxillofac. Implants* **4**, 199-204.

Chambers TJ, Revell PA, Fuller K, Athanasou NA (1984) Resorption of bone by isolated rabbit osteoclasts. *J. Cell Sci.* **66**, 383-399.

Daculsi G, LeGeros RZ, Heughebaert M, Barbieux I (1990) Formation of carbonate-apatite crystals after implantation of calcium phosphate ceramics. *Calcif. Tissue Int.* **46**, 20-27.

Davies JE, Chernecky R, Lowenberg B, Shiga A (1990a) Deposition and resorption of calcified matrix *in vitro* by rat marrow cells. *Cells and Materials* **1**, 3-16.

Davies JE, Lowenberg B, Shiga A (1990b) The bone-titanium interface *in vitro*. *J. Biomed. Mater. Res.* **24**, 1289-1306.

Gomi K, Lowenberg B, Shapiro G, Davies JE (1992) Resorption of sintered synthetic hydroxyapatite by osteoclast-like cells *in vitro*. In: *Transactions, 4th World Biomat. Congress, European Society for Biomaterials, Berlin, Germany*, p 531 (abstract).

Grinnell F (1987) Fibronectin adsorption on material surfaces. *Ann. NY Acad. Sci.* **516**, 280-290.

Gross UM, Strunz V (1977) Surface staining of sawed sections of undecalcified bone containing alloplastic implants. *Stain Technol.* **52**, 217-219.

Gross UM, Strunz V (1980) The anchoring of glass-ceramics of different solubility in the femur of the rat. *J. Biomed. Mater. Res.* **14**, 607-618.

Gross U, Strunz V (1985) The interface of various

glasses and glass-ceramics with a bony implantation bed. *J. Biomed. Mater. Res.* **19**, 251-271.

Gross U, Brandes J, Strunz V, Bab I, Sela J (1981) The ultrastructure of the interface between a glass ceramic and bone. *J. Biomed. Mater. Res.* **15**, 291-305.

Gross U, Kinne R, Schmitz HJ, Strunz V (1988) The response of bone to surface-active glasses/glass-ceramics. In: *CRC Critical Reviews in Biocompatibility*, Vol. 4, CRC Press, Boca Raton, FL, USA, pp 155-179.

Hench LL, Ethridge EC (1982) *Biomaterials - an interfacial approach*. Academic Press, New York, p. 8.

Hench LL, LaTorre GP (1992) Reaction kinetics of bioactive ceramics part IV: Effect of glass and solution composition. In: *Bioceramics*, Vol. 5, Kobunshi Kankokai, Kyoto, Japan, pp 67-74.

Hench LL, Pantano CG, Buscemi PJ, Greenspan DC (1977) Analysis of bioglass fixation of hip prostheses. *J. Biomed. Mater. Res.* **11**, 267-282.

Heywood BR, Eanes E (1987) An ultrastructural study of calcium phosphate formation in multilamellar liposome suspensions. *Calcif. Tissue Int.* **41**, 192-201.

Jarcho M (1981) Calcium phosphate ceramics as hard tissue prosthetics. *Clin. Orthop. & Rel. Res.* **157**, 259-278.

Kim KM (1976) Calcification of matrix vesicles in human aortic valve and aortic media. *Federation Proc.* **35**, 156-162.

Kitsugi T, Yamamuro T, Nakamura T, Kokubo T, Takagi M, Shibuya T, Takeuchi H, Ono M (1987a) Bonding behavior between two bioactive ceramics *in vivo*. *J. Biomed. Mater. Res.* **21**, 1109-1123.

Kitsugi T, Nakamura T, Yamamuro T, Kokubo T, Shibuya T, Takagi M (1987b) SEM-EPMA observations of three types of apatite-containing glass-ceramics implanted in bone: The variance of a Ca-rich layer. *J. Biomed. Mater. Res.* **21**, 1255-1271.

Kooten van TG, Schaakenraad JM, van der Mei HC, Busscher HJ (1991) Detachment of human fibroblasts from FEP-teflon surfaces. *Cells and Materials* **1**, 307-316.

Meenaghan MA, Natiella JR, Moresi JL, Flynn HE, Wirth JE, Baier RE (1979) Tissue response to surface-treated tantalum implants: Preliminary observations in primates. *J. Biomed. Mater. Res.* **13**, 631-643.

Müller-Mai C, Schmitz HJ, Strunz V, Fuhrmann G, Fritz T, Gross UM (1989) Tissues at the surface of the new composite material titanium/glass-ceramic for replacement of bone and teeth. *J. Biomed. Mater. Res.* **23**, 1149-1168.

Müller-Mai CM, Voigt C, Gross UM (1990) Incorporation and degradation of hydroxyapatite implants of different surface roughness and surface structure in bone. *Scanning Microsc.* **4**, 613-624.

Müller-Mai C, Voigt C, Knarse W, Sela J, Gross UM (1991) The early host and material response of bone-bonding and non-bonding glass-ceramic implants as revealed by scanning electron microscopy and histochemistry. *Biomaterials* **12**, 865-871.

Müller-Mai CM, Voigt C, Baier RE, Gross U (1992) Enhanced bone development after implantation of glow-discharge treated surface reactive glass-ceramics. In: *Transactions, 4th World Biomat. Congress*, European Society for Biomaterials, Berlin, p 237 (abstract).

Neo M, Kotani S, Fujita Y, Nakamura T, Yamamuro T, Bando Y, Ohtsuki C, Kokubo T, (1992a) Differences in ceramic-bone interface between surface-active resorbable ceramics: A study by scanning and transmission electron microscopy. *J. Biomed. Mater. Res.* **26**, 255-267.

Neo M, Kotani S, Nakamura T, Yamamuro T, Ohtsuki C, Kokubo T, Bando Y (1992b) A comparative study of ultrastructures of the interfaces between four kinds of surface-active ceramic and bone. *J. Biomed. Mater. Res.* **26**, 1419-1432.

Ohtsuki C, Kushitani H, Kokubo T, Kotani S, Yamamuro T (1991) Apatite formation on the surface of ceravital-type glass-ceramic in the body. *J. Biomed. Mater. Res.* **25**, 1363-1370.

Orly I, Gregoire M, Menanteau J, Heughebaert M, Kerebel B (1989) Chemical changes in hydroxyapatite biomaterial under *in vivo* and *in vitro* biological conditions. *Calcif. Tissue Int.* **45**, 20-26.

Pernot F, Zarzycki J, Baldet P, Bonnel F, Rabischong P (1985) *In vivo* corrosion of sodium silicate glasses. *J. Biomed. Mater. Res.* **19**, 293-301.

Pratt KJ, Williams SK, Jarrell BE (1989) Enhanced adherence of human adult endothelial cells to plasma discharge modified polyethylene terephthalate. *J. Biomed. Mater. Res.* **23**, 1131-1147.

Rich A, Harris AK (1981) Anomalous preferences of cultured macrophages for hydrophobic and roughened substrates. *J. Cell Sci.* **50**, 1-7.

Richardson KC, Jarett L, Finke EH (1960) Embedding in epoxy resins for ultrathin sectioning in electron microscopy. *Stain Technol.* **35**, 313-325.

Sendax VJ, Baier RE (1992) Improved integration potential for calcium-phosphate-coated implants after glow-discharge and water storage. *Dent. Clin. North Am.* **36**, 221-224.

Spurr AR (1969) A low-viscosity epoxy resin embedding medium for electron microscopy. *J. Ultrastruct. Res.* **26**, 31-43.

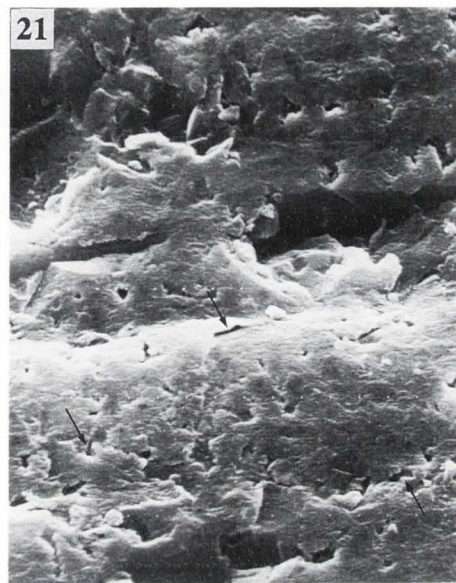
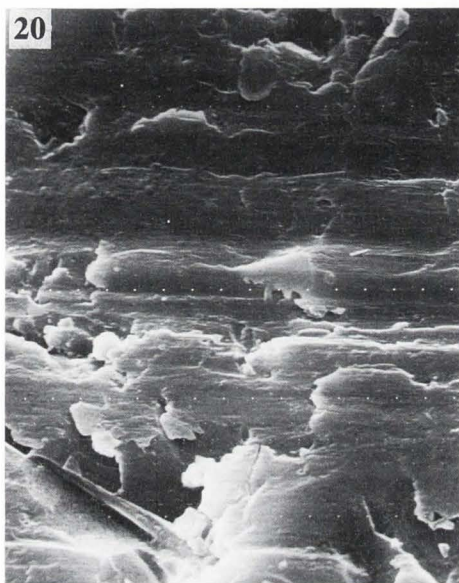
Wennerberg A, Bolind P, Albrektsson T (1991) Glow-discharge pretreated implants combined with temporary bone tissue ischemia. *Swed. Dent. J.* **15**, 95-101.

#### Discussion with Reviewers

**D.M. Brunette:** There is a great difference between the dehydration time of LM samples (24 hours in each concentration of ethanol) compared to the TEM samples (15 minutes). Were the samples trimmed prior to the TEM processing and if so, to what size? What technique was used? Is there a possibility that the interface was disturbed as a result of this procedure?

**Authors:** For LM, femur segments containing total implants were used including the surrounding compact

**Figures 20 and 21.** Surfaces of the non-bonding implant KG y 213 (**Fig. 20**) and bone-bonding implant KG Cera (**Fig. 21**) at two weeks after storage in triple distilled water. In **Fig. 20**: there are no morphological changes of the implant surface. Parallel grooves are due to the sawing process. In **Fig. 21**: tiny pits and clefts are (arrows) are due to storage in water and lead to a partial liberation of the ceramic moiety. SEM. Bars = 10  $\mu\text{m}$ .



bone. A complete implant containing femur segment which was cut in a cortical plane is demonstrated in Fig. 2. To guarantee a sufficient immersion up to the depth of the interface, a prolonged time was required. In the case of the TEM samples, perfusion fixation was first carried out intravitaly in anaesthesia via the abdominal aorta. After the removal of the femur segments with the implant, the tissue was separated immediately from the implants with a diamond-coated rotating disk under constant flow of physiological saline solution until a small rim of tissue was left in contact with the implant surface. This tissue had a width of approximately 1 mm. There were no artifacts. The procedure of preparing the embedded specimens for sectioning has been described in the text. Sectioning was carried out from blocks which had surfaces of less than 1mm<sup>2</sup>.

**D.M. Brunette:** Could there be the possibility that the GD-treatment, storage of implants in water or the histological processing procedure have produced surface irregularities on the KG Cera implants, rather than the irregularities resulting from an active cellular process *in vivo*?

**Authors:** Due to the small number of implants up to now, no implants were investigated directly after GD-treatment avoiding storage in water. Therefore, the possibility that the GD-treatment induces morphological changes on the implant surface cannot be excluded totally, although it seems improbable. This will be elucidated in the near future by performing additional experiments.

Figures 20 and 21 show surfaces of KG Cera and KG y 213 at two weeks after storage in triple distilled water without subsequent sterilization. There were no morphological changes on the non-bonding material as indicated by saw marks. KG Cera shows tiny clefts which were not detected on autoclaved implants which

were not stored in water (Müller-Mai *et al.*, 1991). Additionally, implants which were just sawn and autoclaved were processed for TEM or SEM, respectively (unpublished data). There were no morphological changes on the surfaces of both of the implant materials such as pits or clefts. Saw marks were present on all samples. Therefore, leaching phenomena in fluids, such as water, contribute to the degradation of the material. The role of cells such as macrophages or osteoclasts should be a topic for further investigation. From the results presented here and results of previous experiments cited in this paper, it is obvious that these cell-types at least phagocytose loose implant particles. Whether they support degradation of glass-ceramics by enhanced leaching is not yet clear. In the case of hydroxyapatite, they are able to degrade parts of the materials surface (Müller-Mai *et al.*, 1990).

**D.M. Brunette:** More osteoclasts were found on the KG Cera GD implants than on controls whereas less macrophages were found on the KG Cera GD than on controls. Could the authors speculate how this occurs when macrophages and osteoclasts are derived from the same origin and probably share many properties.

**Authors:** Beside others, one important factor influencing the cellular reaction on materials implanted in bone is the surface rugosity. It was shown in a previous *in vitro* study that implants with higher surface rugosities were colonized by more large, multinuclear cells, which stained positively for acid phosphatase. These cells resembled osteoclasts (Gomi *et al.*, 1992). Therefore, one possible explanation is that rough surfaces induce the fusion of macrophages to become mature osteoclasts. Additionally, chemical differences due to leaching and re-precipitation processes between GD-treated and autoclaved implants might be important and should be investigated.

**J.E. Davies:** To what do you ascribe the cross-banded appearance in the filopodia of the cell in Fig. 6?

**Authors:** Due to the size of the cell and to the diameter of the filopods, it seems to be unlikely that such a cell represents a forming osteoblastic cell.

As described in the text, the GD-sterilized material showed a higher leaching rate as compared to the autoclaved KG Cera implants. It seems possible that such a process leads to high local Ca and P concentrations which can be reprecipitated. This might be one possible explanation for the filopods shown in Fig. 6 some of which resembled cross-banded partially mineralized collagen fibers.

**J.E. Davies:** What is the difference between layer "S" in Fig. 9B and layer "A" in Fig. 10?

**Authors:** The layer on top of the material in Fig. 9B differs in structure (needle-like and roundish structures) and stainability from the bulk phase. Therefore, it is reasonable to say that this layer represents deposited material. Whether this assumed deposition took place during storage in water or during the first days after implantation is not yet clear. In earlier publications, similar afibrillar layers were described on different substrata *in vitro*. Osteoblastic cell-processes were associated with the formation of these surface layers *in vitro* (Davies *et al.*, 1990a,b). Since the morphology of the layers described by Davies *et al.* (1990a,b) is different from the layer demonstrated in Fig. 9B and since we did not observe active cells in association with such a layer, we therefore, assume that the layer was produced by passive processes without involving the action of cells although this possibility cannot be excluded.

Fig. 10A shows a yet non-bonding interface of the GD-KG Cera material at 7 days. This surface layer is rather amorphous and stains as the underlying glass-ceramic. Therefore, it seems that this layer represents a zone on the implant surface which was formerly changed by leaching (loss of ions such as Na, Ca, P etc.) leading to a relative increase of Si in the outermost parts of the implant. As mentioned in the text (*vide supra*), such a Si-rich surface layer is able to incorporate Ca/P and to provide the surface layer acquired for bone-bonding. Between the Ca/P-rich layer (which belongs, in fact, to the implant) and mineralized bone, in many cases, a rather amorphous layer was detected (Gross *et al.*, 1981; Neo *et al.*, 1992a,b; etc.). According to Hench and LaTorre (1992), the amorphous layer presented in Fig. 10A corresponds to stage 5 of the bonding process, i.e., the crystallization of carbonated hydroxyapatite on the implant surface. Active cells were not observed in association with such a layer. A bone-bonding situation is shown in Fig. 10B including the attachment of mineralized collagen fibers to the carbonated hydroxyapatite layer. Therefore, the layers in Fig. 10 seem to represent carbonated hydroxyapatite layers in a yet non-bonding and a bone-bonding zone of the implant surface, whereas Fig. 9 seems to show a rather unaltered surface covered with a layer of unknown source.

**J.E. Davies:** You describe Fig. 10A as a non-bonding region and Fig. 11 as a bone-bonding region. What is the difference between these two?

**Authors:** There seems to be a sequence of morphological events leading to a situation which was called bone-bonding (Hench and LaTorre, 1992). Parts of this sequence are demonstrated in Fig. 10A (establishment of a carbonated hydroxyapatite layer), Fig. 11 (mineralization of such a surface by productive cells, as indicated by the collagen-rich extracellular matrix, which also contains matrix vesicles beneath a part of an osteoblastic cell, collagen starts to become incorporated in this layer), and Fig. 10B (bone-bonding situation with mineralized collagen at top, carbonated hydroxyapatite bonding zone at middle, and implant surface). The rather amorphous part of the bonding zone varies in width depending on the properties of the implant material. It is difficult to detect the exact location of the interface, since the amorphous bonding zone might contain constituents derived from the implant as well as from the surrounding host.

**J.E. Davies:** You explain layer "A" in Fig. 10B as surface reactive layer (Hench *et al.*, 1977; Kitsugi *et al.*, 1987a,b). However you have also seen matrix vesicles associated with this layer (Fig. 11) which cannot be explained by cell degradation since the cell in Fig. 11 looks normal. Neo *et al.* (1992b) also described such a layer on 45S5 glass and on Ceravital-like glass-ceramic KGS which was quite different to the reaction layer which is up to 10  $\mu\text{m}$  thick. They provided no explanation for this, but it would seem to be similar to the cement-like layer which we have described (Davies *et al.*, 1990a) which is also made by cells before they become fully functional osteoblasts. Why have you chosen to exclude this possible explanation?

**Authors:** It was already demonstrated that a Ca/P-rich layer consisting of apatite crystals which are different from those of the bone in size, shape, and orientation forms on KG Cera-type glass-ceramic KGS, i.e., these crystals are small and granular (Neo *et al.*, 1992a). This layer contains carbonated hydroxyapatite with small crystallites and is defective in structure (Ohtsuki *et al.*, 1991). Layers of comparable morphology were observed occasionally on hydroxyapatite (Daculsi *et al.*, 1990; Müller-Mai *et al.*, 1990; Neo *et al.*, 1992b), but were missing on resorbable ceramics which were therefore considered to bond to bone mechanically, e.g.,  $\text{CaCO}_3$ -ceramic or  $\beta$ -tricalciumphosphate (Neo *et al.*, 1992a). Hydroxyapatite showed bonding interfaces with or without such an intervening bonding layer (Müller-Mai *et al.*, 1990; Neo *et al.*, 1992b). Therefore, the development and thickness of an intervening layer depends on the material properties at a given site, e.g., surface roughness, solubility, and other factors.

Glass-ceramics exchange ions with the host tissue. Due to different structures of bone apatite crystals and crystals of the intervening layer, other processes, namely, leaching and reprecipitation seem to be involved.

The conditions are different in normal bone formation.

Cells producing layers of similar morphology, which were observed on different non-bonding substrata with smooth surfaces *in vitro* (Davies *et al.*, 1990a,b), were not observed in the study presented here. Therefore, such processes might occur before the third day after implantation. Different mechanisms might be operative on different types of materials, e.g., the bond via an apatite-like intervening layer as demonstrated here or the bond via inserting collagen fibers which later on become mineralized as demonstrated earlier (Müller-Mai *et al.*, 1990; Neo *et al.*, 1992a). Matrix vesicles (Fig. 11) were only focally observed in association with an intervening layer which was covered with a collagen-rich ECM. This layer was already partially mineralized. It seems that these vesicles are operative in accelerating mineralization of the collagen-rich ECM, but are not important to establish the carbonated intervening layer.

**Reviewer III:** The authors use, for reasons we all know, three animals per group and apply a very simple two-dimensional histomorphological measurement technique which was not described. This is at the very extreme limit of statistical methodology. In the results, one of the KG Cera implant sections was stated to yield 100% bone contact at 28 days, yet in the Table 92.9% was the average and the standard error of mean (S.E.M.) less than one, these figures do not add up. What relevance does the S.E.M. have to the sample statistics presented here? More sophisticated 3-D histomorphological packages have been available for 20 years to use on this problem.

**Authors:** The aim of the histomorphometric measurements was to quantitate the bone-implant contact according to day and method of sterilization. Statistical tests were performed using the 4 slices of each specimen since only a limited number of implants was available. Three-dimensional packages were not used since, due to the sawing process, part of the implants was lost and the reconstruction would, therefore, be speculative.

**Reviewer III:** Some people believe strongly in matrix vesicles, others strongly not. Both groups have good arguments. Until some definitive proof is found, perhaps dogma should not be stated as fact!

**Authors:** Due to many publications in the relevant literature, it becomes more and more clear that matrix vesicles play a role under certain circumstances, e.g., mineralization of collagen-rich extracellular matrix. Therefore, the authors do not wish to change the text passages dealing with matrix vesicles.

**Reviewer III:** The authors have presented some statements on the physics of the interface which are imprecise. A good definition of surface energy does not exist and in any case, there is great difficulty in making measurements. GD-treatment surely does much more than change the wettability? Cell attachment strengths are not correlatable with water angle measurements as this is to coarse a measurement to tell us anything about the surface.

**Authors:** New implants were prepared already for surface analysis and leaching experiments. This will be the topic of another study and publication.